JCTC Journal of Chemical Theory and Computation

Article

pubs.acs.org/JCTC

Mechanism of Stapled Peptide Binding to MDM2: Possible Consequences for Peptide Design

Adelene Y. L. Sim,*[,†] Thomas Joseph,[†] David P. Lane,[‡] and Chandra Verma*[,†,§,∥]

[†]Bioinformatics Institute (A*STAR), 30 Biopolis Street #07-01, Matrix, Singapore 138671

[‡]p53 Laboratory (p53Lab, A*STAR), 8A Biomedical Grove, #06-06, Immunos, Singapore 138648

[§]School of Biological Sciences, Nanyang Technological University, 60 Nanyang Drive, Singapore 637551

[∥]Department of Biological Sciences, National University of Singapore, 14 Science Drive 4, Singapore 117543

Supporting Information

ABSTRACT: MDM2 is a negative regulator of p53. The N terminal domain of MDM2 interacts with a helical region of the transcriptional activation domain of p53. Stapled peptides have been designed to mimic this interaction, in order to inhibit p53-MDM2 binding and thereby activate the p53 response. Here, we studied how the helical segment of p53 or a stapled peptide (re)binds to MDM2 as it is systematically displaced from the MDM2 binding pocket. Depending on its sequence, presence of staple, and/or a C-terminal tail, the peptide approaches MDM2 differently and not exclusively via the crack propagation mechanism proposed previously for p53. The presence of an interacting staple appears to reduce the peptide's sensitivity to mutations of key hydrophobic residues of p53, and this could pave the way for increased diversity in sequence design of stapled peptides used in inhibiting the p53-MDM2 interaction. We further found that the presence of a hydrophobic staple in the peptide-MDM2 interface tends to trap a network of water molecules prior to binding. The release of these structured waters would then reduce the entropic penalty upon peptide binding.

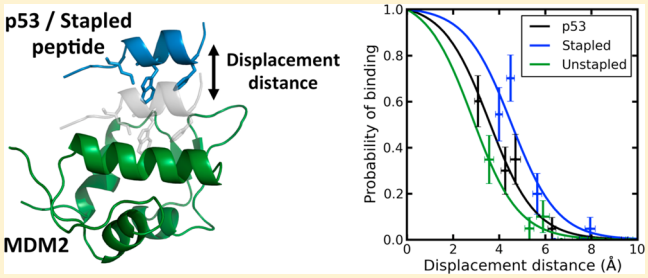

INTRODUCTION

p53 is a tumor suppressor protein that is involved in a highly intricate network of processes, and disruption of its function (directly or indirectly) occurs in most human cancers.[1] When cells are under stress, p53 activates cell-cycle arrest, senescence, apoptosis, and modulation of autophagy.[2,3] p53 is negatively regulated by the E3 ubiquitin ligase MDM2: MDM2 controls p53 concentrations in cells by binding to p53 and regulating its ubiquitination.[4,5] MDM2 amplification has been observed in more than 10% of 7700 human tumors in various locations.[6] An upregulation in MDM2 causes p53 concentrations to fall due to increased ubiquitin-dependent proteolysis.[7]

MDM2 and p53 interact with each other via two sites: i) the N-terminal domain of MDM2 with the transcriptional activation domain (TAD) of p53[8] and ii) the acidic domain of MDM2 with the DNA binding domain of p53.[9,10] From X-ray crystallographic data, the N-terminal domain of MDM2 was shown to form a hydrophobic pocket that encapsulates a small helical region of the p53 TAD.[8] Three key hydrophobic residues (F19, W23, and L26) of p53 are crucial for this interaction, and the mutation of any of these residues leads to significant reduction in p53 binding to MDM2.[11−13] In tumors where MDM2 is amplified, inhibiting the p53-MDM2 interaction would increase the p53 concentration in cells for suppression of tumor growth. Hence there is much interest in identifying small molecule inhibitors of this interaction. Of the small molecule drugs discovered that inhibit the p53-MDM2 interaction, the most promising for cancer therapeutics appears to be Nutlin, whose derivatives are currently in clinical trials.[3,14,15]

The usefulness of small molecule drugs is limited though, as only a minority (∼10%) of human proteins have hydrophobic pockets at their surface that can bind to small molecule drugs with high specificity and affinity.[16,17] Small proteins, or peptides, are potentially a more versatile class of next-generation drugs that can mimic diverse types of protein−protein interactions.[18] However, such peptides are typically highly flexible, resulting in low binding affinity and selectivity, as well as vulnerability to degradation by proteases: properties contributing to poor drug bioavailability.[19] By attaching a covalently linked hydrocarbon chain to the peptide − in a process known as stapling − the peptide is rigidified, and its resistance to degradation is increased,[20] and in some cases cellular uptake is enhanced.[21,22] Additionally, since a stapled peptide has diminished conformational diversity, the entropic cost of peptide binding is reduced.[23]

Stapled peptides designed to bind to MDM2 have been shown to be effective inhibitors of the p53-MDM2 interaction.[22,24,25] Despite these experimental findings, there

Received: October 23, 2013
Published: March 6, 2014

   dx.doi.org/10.1021/ct4009238 | J. Chem. Theory Comput. 2014, 10, 1753−1761

are still various aspects of how the staple affects peptide binding that are not well understood. The paucity of detailed structural data on the interactions between stapled peptides and MDM2 and the lack of complementary dynamic information have both contributed to the limited structural understanding of the effects of stapling on peptide binding affinity and dynamics.

Previous computational work in our group studying the interaction of stapled peptides to MDM2 suggested that under certain stapling conditions, the hydrophobic staple interacts with MDM2, thereby increasing the interaction interface and the associated binding free energy. The binding free energy is less favorable if the staple is positioned such that it is exposed to solvent where the staple-MDM2 interaction is considerably weakened if not absent.[26] This structural modeling was later validated by X-ray crystallography.[24] Similar enhancements in affinity resulting from the interactions between the staple and the target protein surfaces have been reported for other systems.[27−29]

This previous computational study was based on equilibrium simulation data of peptides bound to MDM2 and therefore lacks information about how the peptides approach MDM2 prior to binding. (Although earlier reported work probed how p53 approached and bound to MDM2,[30] it was based on a small number of simulations and did not consider stapled peptides.) With a detailed understanding of the mechanism(s) by which a stapled peptide accesses the binding pocket in MDM2, we can identify residues that were previously not known to be dispensable for stapled peptide binding. Besides binding affinity, peptide aqueous solubility and cell permeability are key properties to consider when optimizing stapled peptides for *in vivo* therapy.[16] By identifying less critical residues that can potentially be mutated, many more sequence options are available for designing peptides with improved druglike attributes.

To this end, we conducted extensive molecular dynamics simulations of peptides displaced from their bound conformations and observed how they rebind (if at all) to MDM2. The list of stapled and unstapled peptides studied is compiled in Table 1. The nature of our setup allows us to probe the behavior of the peptides and MDM2 just as binding is about to take place: i.e. the MDM2 hydrophobic pocket is open and ready for peptide binding, while the peptide has already adopted the helical form required for binding. This latter assumption is reasonable since the peptide region used in our study has been found to be mostly helical (residues 19−25 of p53)[31,32] although most other regions of the p53 N-terminus are largely unstructured[33−35] prior to protein binding.

Table 1. Summary of Peptides Studied[a]

name	sequence (*: staple)	comments
p53	Ac-ETF**S**DL**W**KLLPEN-NH_2	
Stapled	Ac-TS**F***EY**W**AL**L***-NH_2	
Stapled-LTrp	Ac-TS**F***EY**W**AL**L***-NH_2	L-form 6-Cl modified **W**
Stapled-DTrp	Ac-TS**F***EY**W**AL**L***-NH_2	D-form 6-Cl modified **W**
Unstapled	Ac-TS**F**AEY**W**AL**L**S-NH_2	
ST3	Ac-LSQ*T**F**SDL**W***LLPEN-NH_2	
ST5	Ac-LSQET**F***NL**W**KLL*QN-NH_2	

[a]Key hydrophobic residues for p53-MDM2 binding (F19, W23, and L26, based on full p53 sequence) are indicated in bold. Throughout the text, the residue numbers labeled for these key residues will be based on the full p53 sequence.

The current study begins to dissect out some details of the binding mechanics of p53 and its analogues to MDM2. We omitted Nutlin from our study as the binding mechanisms for peptides and small molecules could be very different and hence challenging to compare. This becomes even more poignant as recent studies have shown that there appears to be a secondary Nutlin binding site[36] that makes interpreting the binding mechanism of Nutlin to the main site complicated and thus is being explored separately.

MATERIALS AND METHODS

Peptide Only Simulations. Peptide only simulations were conducted using the GPU accelerated version[37,38] of AMBER11/12 simulation package.[39] Each peptide was capped at the N- and C-termini with acetyl and NH_2 moieties, respectively, and placed in a waterbox with edges at least 8 Å away. Each system was energy minimized and then heated to 300 K for 10 ps. Six independent 50 ns simulations were next run for each peptide, and in all cases the systems were deemed to have equilibrated by 5 ns, and statistics were taken only from subsequent frames. The relative side chain distances were determined based on the centers of masses of side chain heavy atoms of residues F19, W23, and L26 of p53 (or their equivalent; numbering is based on full-length p53 sequence). All simulations were conducted with the AMBER-99SB force-field[40] and the TIP3P water model.[41] Electrostatics were handled with the particle-mesh Ewald approach,[42] while all other nonbonded interactions were evaluated with a cutoff of 12 Å. A time step of 2 fs was used, and SHAKE[43] was implemented to constrain all bonds involving hydrogen atoms.

Approach Simulations. Each peptide was displaced in the direction connecting the centers of masses of MDM2 and the peptide to distances of 5−12 Å. For p53, the crystal structure of the p53-MDM2 bound state (PDB id 1YCR[8]) was taken as reference, while equilibrated structures, generated as described previously,[26] were used as references for the other peptides studied.

Water molecules and counterions were added to the simulation boxes such that the protein atoms were at least 8 Å away from the box edges. Each system was first heated and equilibrated for 10 and 40 ps, respectively, with both MDM2 and peptide backbones constrained. Then 2 ns runs were conducted without constraints at 300 K. It was observed that in these equilibrium runs, from 20 ps onward, the system was equilibrated based on water density. Hence in all cases, we used this 20 ps frame as the starting conformation: the initial displacement illustrated in Figures 2, 4 and Figure S6 refer to the backbone RMSD (considering only residues E17 to P27 based on the full-length p53 sequence, or their equivalent) of this starting peptide conformation relative to the bound conformation, with MDM2 backbone-aligned. Twenty independent simulations were run for each center of mass displacement for better statistics. Peptide termini were capped as before, and MDM2 was capped at the N- and C-termini with acetyl and N-methyl moieties, respectively. All simulations were conducted with the same force-fields, time step, and nonbonded interaction cutoff as for the peptide-only simulations.

For each simulation, the displaced peptide is considered to have rebound if:

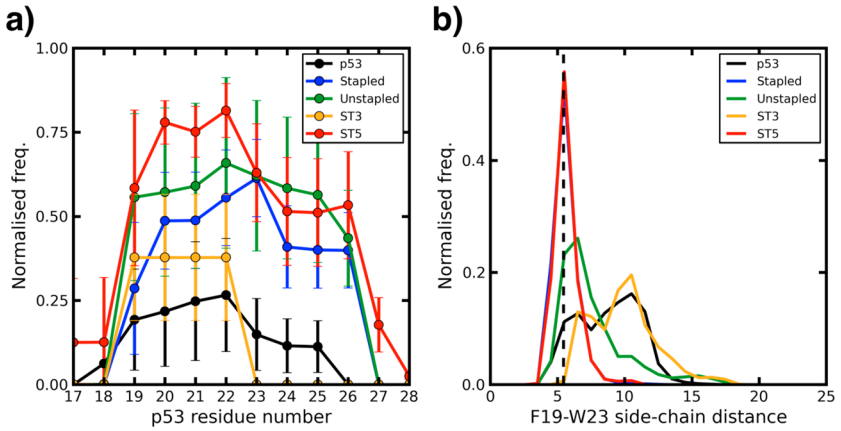

Figure 1. (a) The normalized fractional alpha-helicity as a function of residue number (aligned to p53 sequence). The extent of increased helicity from peptide stapling depends on the location of the staple. The Unstapled peptide sequence improves helicity relative to p53. (b) The key hydrophobic residues maintain their relative positions identical to that found to the bound p53 (black dashed line) only for certain stapled conditions (Stapled and ST5).

1. The peptide backbone RMSD is within 2.0 Å from the native (considering only residues E17 to P27 or their equivalent, with MDM2 backbone-aligned)
2. The peptide stays within 2.0 Å of the native for at least a total of 500 ps (does not have to be continuous)
3. Each continuous time window where the peptide backbone RMSD is within 2.0 Å is at least 100 ps. This criterion screens out situations where the peptide vacillates close to the bound conformation but fails to properly sit in the binding pocket. The length of each continuous time window, regardless of whether the peptide is considered "bound", was defined as "dwell time" in Figures 2 and 4.

The probability of binding then simply is the percentage of times the peptide rebinds out of the twenty independent runs at a given center of mass displacement. To estimate the errors in Figures 2a and 4a, data for each center of mass displacement were grouped together and bootstrapped. For each particular distance, from the set of twenty independent simulations, a "new" set of twenty was chosen, with replacement, and the average displacement distance and binding probability recorded. This bootstrapping was repeated, to obtain 1000 sets of bootstrapped data. That is, we obtained 1000 data sets of binding probabilities versus displacement distances.

For each bootstrapped data set, the scattered data points were fitted to the sigmoidal function

$$\text{Probability, } P(x) = \frac{1 + e^{-a}}{1 + e^{x-a}}$$

where x is the displacement distance, and a is a fitting parameter. The standard deviations of the bootstrapped displacement distance and probability of binding are illustrated as error bars in Figure 2a. Standard deviations in the fitting parameter a and $x_{1/2}$ (the displacement distance where the rebinding probability was 0.5) are shown in Table S1.

The dwell times and times taken for peptide binding were similarly bootstrapped.

Mutagenesis Simulations. Mutations to peptides were carried out using the Mutagenesis Wizard in PyMOL.[44] The bound conformations of the mutated peptides were assumed to be similar to the wild type case: this allows us to easily define the bound state without having to conduct extensive equilibrium simulations for the different mutations.

Binding Mechanism. The binding mechanism adopted by each peptide for every independent simulation was visually determined. While the mechanisms were sorted discretely, in reality the peptide binding could occur with a combination of mechanisms. Cases where a single dominant mechanism was observed were then sorted accordingly. If the peptide binds via a mixture of mechanisms, that particular binding mechanism was then classified as "other" as it is challenging to quantitatively distinguish the percentage contributions of the different mechanisms.

Our straightforward cataloging of the different mechanisms highlights salient peptide binding features. Hence we can gain insight into how the peptide's sequence, length, and presence of staple affect how it binds to MDM2 simply by comparing the distributions of binding mechanisms.

RESULTS AND DISCUSSION

Effect of Staple on Peptide Helicity and Relative Key Residue Positions. To further understand the effects of peptide sequence and stapling, we looked at some of the peptides in isolation. Simulations by Guo et al.[45] suggest that peptide stability and structural flexibility depends on the position of the staple, with the latter being a better indicator of peptide binding to MDM2 than absolute peptide alpha-helicity. Similarly and additionally, we observe in our simulations of the isolated peptides, that the alpha-helicity of a peptide not only depends on the presence/position of the staple but also on the peptide sequences (see Figure 1a; see also atomic fluctuation plots in Figure S1; frequencies of other helical forms are additionally shown in Figure S2). Since we are further interested in the ability of the peptide to (re)bind to MDM2, we compared the relative positions of key hydrophobic residues (based on distances between centers of masses of key residues; see Figure 1b and Figure S3).

Stapled and Unstapled have identical sequences and differ from each other only by the presence of a staple. Both show higher alpha-helicity throughout the peptide than p53 (Figure 1a). However, the staple plays a key role in maintaining the relative side-chain positions: Unstapled has similar alpha-helicity as Stapled but shows much more variation in distances between side chains of key hydrophobic residues (Figure 1b and Figure S3). The distances between the centers of masses of the key hydrophobic residues in Stapled are better preserved

dx.doi.org/10.1021/ct4009238 | J. Chem. Theory Comput. 2014, 10, 1753−1761

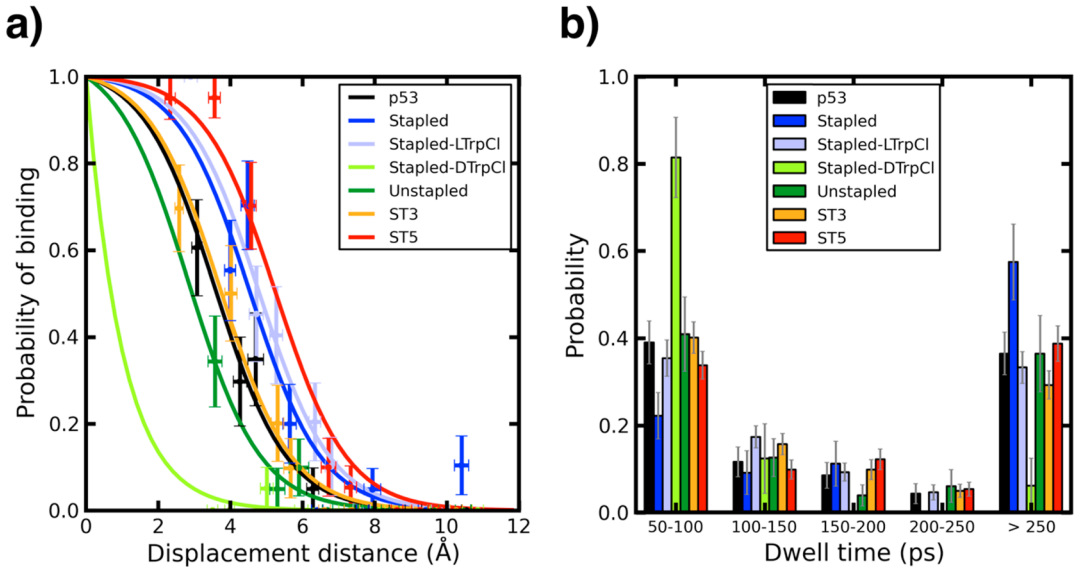

Figure 2. (a) Probability that the different peptides rebind (see Materials and Methods for definition) to MDM2 as a function of displacement distance (taken as initial backbone RMSD after equilibration). For visualization, sigmoidal fits to the data are also shown. ST5, Stapled-LTrpCl, and Stapled rebind with higher propensity than p53, while ST3 and Unstapled rebind as a function of displacement distance similar to p53. Stapled-DTrpCl is essentially unable to rebind when displaced. Error bars are obtained from bootstrapping (see Materials and Methods). (b) The time ("dwell time") the peptide fluctuates within the bound state (≤2 Å peptide backbone RMSD). Statistics were gathered from all independent simulations and normalized by number of "bound windows" (see Materials and Methods).

because the key residues tend to move in a correlated fashion due to the constraints imposed by the presence of the staple. However, such synchronized movement is not apparent for all stapled peptides. Comparing ST3 and ST5, we observe that the location of the staple affects the degree of alpha-helicity and the relative positions of key residues (Figure 1b and Figure S3).

Hence it appears that when optimizing the location and length of the staple, it is important to consider both the preserved helicity as well as the effects of the staple on the packing of hydrophobic residues. The relative orientations and locations of the latter can significantly affect the fit of the peptide into binding pockets. Next we explore how stapling affects complex formation between peptides and MDM2.

Sensitivity of Peptide Binding to Approach Distance: Indirectly Probing the Near-Native Energy Landscape. Previous approach simulations have given us insights into binding of p53 to MDM2.[30,46] However, these simulations were conducted only on a p53 peptide, with a limited set of initial peptide displacement distances. In order to better understand the effects of stapling (absence/presence and location) and sequence on peptide binding to MDM2, we need a more systematic and comprehensive protocol that allows us to compare binding likelihoods and mechanics across different peptides.

Ideally, such a protocol would involve extensively exploring the energy landscapes of the different peptides as they approach MDM2. That way, one can compare the free energy landscapes of the different peptides to see how specific features could affect the binding energy landscape. A broad, smooth, and deep energy basin around the bound conformation favors peptide binding − even if the peptide is far from the binding pocket, the nature of the energy basin ensures that it approaches the bound conformation with high affinity.[47] The converse is true for a narrow energy basin. Furthermore, if the energy landscape near the bound state is rugged, the peptide likely gets trapped in different local energy minima prior to binding, and therefore the peptide is less likely to bind.

However, extensive exploration of energy landscapes is notoriously challenging due to sampling constraints. Hence we attempted to indirectly probe the nature of the energy basins around the peptide-bound conformations. To do this, for each peptide, we conducted twenty independent approach simulations for a range of perturbation distances. Then the distributions of rebinding probabilities (see Materials and Methods) as a function of distance gives an indication of the nature of the energy landscape funnel, as the peptide approaches MDM2. Although such distributions are simplified models of the true energy landscapes, they do provide a comparative analysis of the different peptides.

Our results reveal trends that are qualitatively similar to experimentally determined trends in dissociation constants (K_d) probed by fluorescence anisotropy.[22,25] From Figure 2 and Table S1, most stapled peptides rebind to MDM2 better than p53. ST3 rebinds with similar propensity to p53, perhaps due to its staple being unable to enforce the same level of constraint on relative key residue positions as for other staples (see Figure 1). Replacing W23 (based on p53 residue numbering) with a 6-chloro-L-tryptophan improves rebinding propensity of the peptide only marginally over Stapled (compare Stapled-LTrpCl with Stapled in Figure 2); experimental data suggests a more marked improvement in binding.[25] This likely originates from improved van der Waals interactions between the peptide and MDM2 with the addition of Cl to W23.[25,48,49]

Changing the isomeric form of 6-chloro-tryptophan from L to D (Stapled-DTrpCl in Figure 2) inhibits any rebinding in our simulation. Experimental findings indicate that while Stapled-DTrpCl interacts with MDM2 moderately, it is unable to reinstate p53 activity in the cell.[25] In the D-isomer, the N−H on W23−Cl is oriented in the opposite direction and is therefore unable to hydrogen bond with L54 of MDM2 that stabilizes the p53-MDM2 interaction. We also found that the D isomeric

dx.doi.org/10.1021/ct4009238 | J. Chem. Theory Comput. 2014, 10, 1753−1761

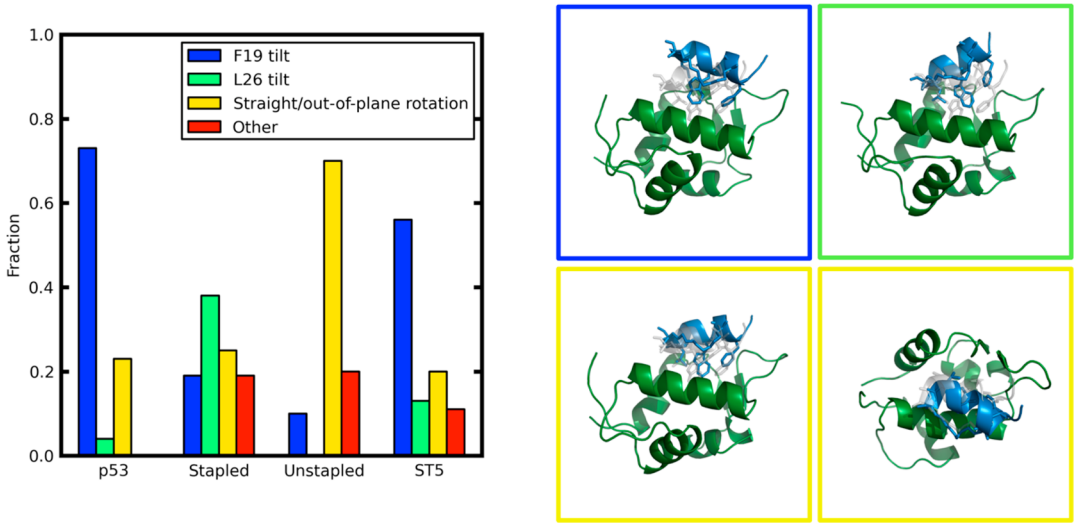

Figure 3. Binding mechanisms for p53, Stapled, Unstapled, and ST5. p53 preferentially binds MDM2 by tilting in the F19 direction. The presence of the staple changes the binding mechanism of Stapled compared to p53, as the increased helix stability enables the peptide to tilt or orient to bind MDM2 more readily. Differences observed in MDM2-binding for Unstapled compared to p53 suggest that the sequence and length of the peptide likely affects its binding mechanism too.

form is unstable, and when Stapled-DTrpCl is simulated in isolation, the 6-chloro-tryptophan tends to rotate about its dihedral angle χ_1, away from its starting orientation (Figure S4). Additionally, F19 samples other dihedral angle states frequently, and in some cases χ_1 even rotates by ~100° from the starting configuration (Figure S4). The lack of Stapled-DTrpCl rebinding to MDM2 in our simulations is likely attributable to all these factors, but our results are clearly inadequate to explain the experimental results of Brown et al.[25]

Another aspect of rebinding that we can quantify is the time taken for the peptide to bind. We observed that the times taken for the peptides to bind to MDM2 increased with initial displacement distances in a manner similar for all peptides (Figure S5), suggesting that the approach time could therefore be diffusion limited.

Additionally, we can observe how long the peptide stays bound once it rebinds. Our criterion for evaluating this "dwell time" is defined in Materials and Methods. Note, however, that our measurement of dwell time is limited by the 2 ns total simulation time for each independent trajectory. The dwell time gives us additional information about how well the peptide actually sits in the binding pocket, and how much the peptide fluctuates about the "bound" state; the aforementioned rebinding propensity only considers whether the peptide rebinds or not. Figure 2b shows that Stapled has a higher proportion of longer dwell times compared to p53, which has similar dwell time distributions as Unstapled. Conversely, Stapled-DTrpCl vacillates around the binding pocket but is unable to bind for a long, continuous stretch of time. These dwell time results likely will be related to k_{on} and k_{off} rates; however, it is challenging to draw direct kinetic information from our simulation setup.

Binding Mechanisms. Previous work suggested that native p53 binds sequentially to MDM2, with F19 being the first key hydrophobic residue entering the MDM2 binding pocket, followed by W23 then L26, in a manner analogous to crack propagation.[30] Our extensive set of approach simulations indicated that the initial F19 binding does take place in most cases for p53 (see Figure 3). This binding mechanism is often facilitated by initial hydrogen bonding interactions between the backbone of F19 and/or E17 with the side chain of Q72 on MDM2. Both hydrogen bonds help to keep the position of the peptide relative to MDM2 for initial F19 entry into its hydrophobic pocket (consisting of MDM2 residues I61, M62, Y67, V75, and V93), which subsequently molds around F19, clasping the peptide on one end before W23 falls into its pocket and forms a hydrogen bond with the backbone of L54 of MDM2. L26 enters its pocket after the "encapsulation" of F19 and W23 by MDM2, respectively.

The p53 peptide rarely binds via a L26 tilt, and this likely can be attributed to its long, unstructured C-terminal tail that causes steric clashes with MDM2 should L26 try to enter the hydrophobic pocket first. We also observed this lack of L26 tilting for other peptides with long C-terminal tails (discussed later).

On the other hand, Unstapled appeared to preferentially enter the pocket without tilting in the F19 or L26 pockets. In comparison with p53 binding mechanisms, this observation suggests that the sequence of the peptide and/or the absence of a longer C-terminal (residues beyond L26 of p53) could all result in somewhat differing binding mechanisms. In the absence of a staple, Unstapled is more flexible and able to induce fit into the binding pocket without tilting.

In this no tilting or straight/out-of-plane rotation mechanism, unlike in the cases of F19 or L26 tilt, none of the three key residues tends to bind first, but rather the peptide appears to be attracted to its binding pocket via a generic hydrophobic interaction that is often expedited by hydrogen bonding of the N-terminus of the peptide with MDM2. The backbone of E17 (p53; T17 for Stapled and Unstapled) and/or the backbone of F19 occasionally interact(s) with the side chain of Q72 of MDM2. Subsequently, once the peptide is in the proximity of the binding pocket, it rotates and adjusts to the MDM2 binding pocket (which in turn also morphs to the peptide). Usually the hydrogen bonding between W23 and L54 of MDM2 secures the position of the peptide relative to MDM2 during the adjustment phase. We observed less of this binding mechanism for p53, likely due to steric constraints imposed by the C-terminal tail.

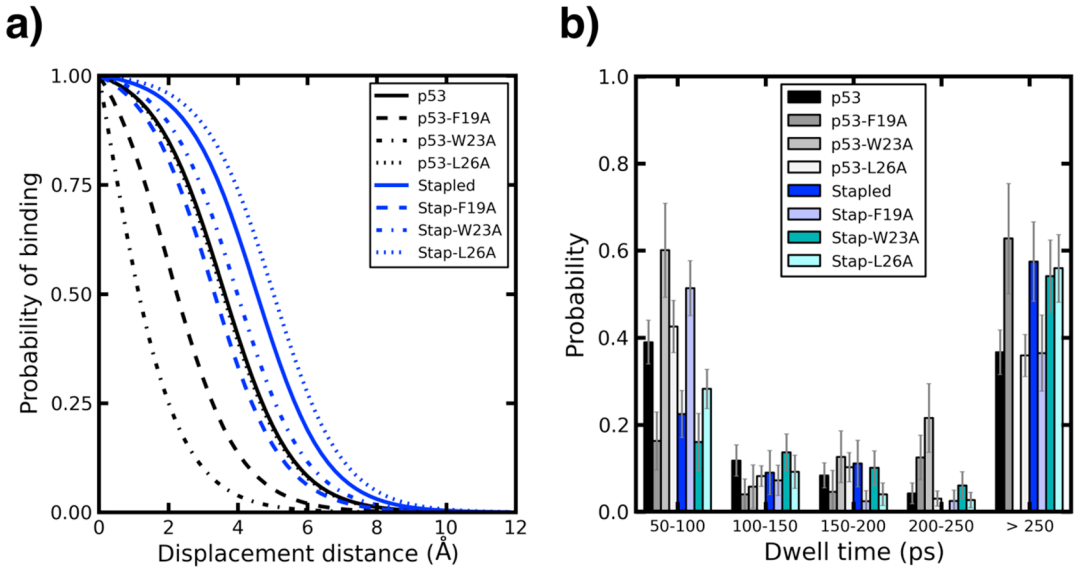

Figure 4. Effect of mutation of key residues on rebinding propensity (a) and stability (b). Rebinding for Stapled is at least as efficient as p53 regardless of key residue mutations. F19 appears to be most crucial to rebinding probability, while the L26A mutation plays a less pronounced role in modifying binding affinity for Stapled. For p53, W23A mutation makes the most significant change in rebinding probability and peptide dwell time. Data points were omitted in (a) for clarity.

The added rigidity imposed by the staple and the absence of a long C-terminal tail causes Stapled to bind with both the F19 and L26 tilts. The L26 tilt mechanism is analogous to a mirror image of the F19 tilt: L26 first enters its binding pocket (albeit this fit is less snug than F19's) then hydrogen bonding between W23 and L54 of MDM2 helps secure the peptide into the binding pocket before F19 binds. In some instances, however, a no tilt binding mechanism is still detected for Stapled, and this mechanism is accommodated by rotation or displacement in the out-of-plane direction (Figure 3). Conversely, ST5 binds predominantly in a manner identical to p53, even though its staple is similarly positioned as Stapled. This confirms our hypothesis that the long C terminal tail affects the binding mechanism adopted by the different peptides.

Hence the F19 crack propagation binding mechanism previously proposed[30] is not general and depends on peptide length as well as on the presence of a staple. Our results, taken together with previous experimental observations suggesting that shorter p53-derived peptides bind more tightly to MDM2,[50] point to peptide length as another tunable parameter for therapeutic peptide drug design.

The distribution of binding mechanisms appears to show some dependence on initial perturbation distance (not shown), but unfortunately it is not possible to study this systematically due to poor statistics from the reduced number of binding incidences as the initial displacement increases.

A Peptide with Staple Forming Part of the Binding Interface Is More Robust to Key Residue Mutations. From our observations of binding mechanisms, we expect that the dependence of Stapled on key residue mutations would be different from that of p53. That is, since Stapled can bind to MDM2 using several approaches, it could be more resilient to F19A, W23A, and L26A mutations compared to p53. We compare the effects of sequence mutations on peptide binding next.

The staple increases the peptide-MDM2 binding interface, and this hydrophobic interaction contributes ∼−7 kcal/mol to the binding energy, similar in magnitude to that from each of the key hydrophobic residues.[26,51] Hence it is plausible that the presence of the staple will make the binding of Stapled less dependent on the existence of the three key residues F19, W23, and L26. We tested this using our approach simulation protocol as before, while assuming that, relative to MDM2, the backbone of the bound conformation of each mutated peptide is identical to that of the wild type case.

For single mutations, the F19A mutation affects rebinding propensity of the stapled peptide most significantly (Figure 4a and Table S1), and when the peptide does rebind, binding is less tight, and the peptide fluctuates about its bound conformation more noticeably (see Figure 4b). From Figure 5, we observe that the stapled peptide with the F19A mutation

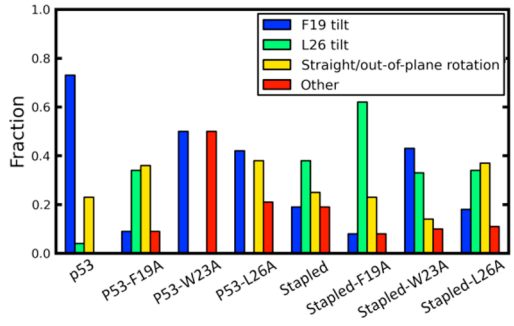

Figure 5. When mutations occur to key residues of p53 or Stapled, the peptide binds preferentially via different mechanisms to compensate for the loss of key residues.

compensates for the loss of F19 by preferentially binding via a L26 tilt, much more than for the wild type Stapled. This is likely due to the absence of the F19 anchor that could help in p53 binding via a crack propagation mechanism[30] as discussed previously.

The W23A mutation decreases rebinding propensity slightly but does not seem to affect the dwell time of the stapled peptide. This is surprising because the absence of hydrogen bonding between W23A and L54 of MDM2 should destabilize

the peptide in the binding pocket. The additional binding interface provided by the staple might have helped to mitigate this loss of hydrogen bonding, resulting in no significant decrease in peptide dwell time. The L26A mutation showed negligible effect on rebinding statistics and mechanics.

As a comparison, we also performed single mutations on p53. The best sigmoidal fits to the simulation data imply that single mutations to p53 cause more significant decreases in rebinding probability than single mutations do to the stapled peptide (Table S1). Our approach simulations are qualitatively consistent with experimental data[13] suggesting that the W23A mutation caused the most significant change in binding affinity of p53 peptide, among all three key residues.

We additionally observed that when pairs of key residues were simultaneously mutated, if either F19 or W23 is present, the stapled peptide was still able to rebind to MDM2 in a distance-dependent manner that is at least similar to that of native p53 (Figure S6; binding mechanisms shown in Figure S7). When both F19 and W23 were mutated to alanine, and even when all three key hydrophobic residues (F19, W23, and L26) were mutated, the peptide was still able to rebind, with the help of the interacting staple, albeit with lower propensity than the native p53 peptide. Single mutations of F19A and W23A in p53 reduced binding propensity more drastically than the triple mutation for Stapled.

The MDM2 N-terminal binding pocket can morph to accommodate the peptide or small molecule drug that it is bound to (for example as revealed by comparison of the binding pockets in the p53-MDM2 structure[8] with the MDM2 structures bound to small molecules[52,53]). Hence, despite the loss of key hydrophobic residues in mutant peptides, MDM2 is, through the process of induced fit, still able to maximize (albeit small) van der Waal's interactions. This, together with compensatory interactions between the staple and MDM2, appears to be adequate to allow binding of even the triple mutant stapled peptide to MDM2. These studies combined with observations that the MDM2 pocket is quite pliable[36,53] suggest promiscuity in the interactions of MDM2; experiments revealing the motifs from diverse proteins in the cellular context[54] are eagerly awaited.

With each of the key residues (and even combinations of residues) less crucial for peptide binding, we have more opportunities for designing peptide sequences that both enhance binding to MDM2 and promote cell permeability. This observation will likely also hold for peptide binding to other systems, in cases where the staple is part of the binding interface.

Water-Mediated Peptide-MDM2 Interactions. Water is vital in biology[55,56] and is crucial in facilitating the attraction of hydrophobic protein−protein interfaces (e.g., see refs 57−60). We noticed that when the hydrophobic staple is part of the protein−protein interface, it tends to cause an intricate network of waters molecules to be trapped between the staple and MDM2 (albeit in some instances only one trapped water was seen; see Figure 6). This network of waters observed might be analogous to the clathrate-like/pentagon ring water structures detected around other hydrophobic residues.[61−63] Such a water-trapping feature was observed also for ST5 but not for p53 or Unstapled or stapled peptide ST3 that has its staple oriented away from MDM2 (data not shown), suggesting that the staple has to come into close proximity with MDM2 in order for the water network to be formed.

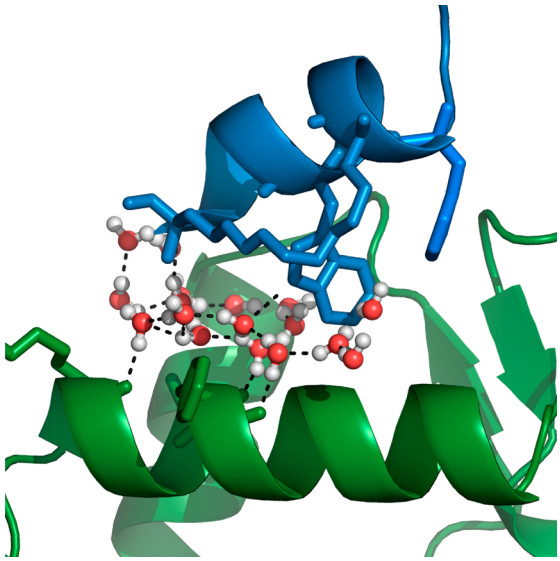

Figure 6. An intricate water structure formed between the staple and MDM2 for Stapled. Water molecules are shown in ball and sticks (red for oxygen and white for hydrogen), while the key hydrophobic residues of Stapled (F19, W23, and L26 based on full p53 sequence) and the staple are shown in sticks. Residues on MDM2 that interact with the water network are also highlighted in stick format.

The N−H dipole on the side chain of W23 hydrogen bonds with a water molecule that is part of the more extensive water network trapped between the staple and MDM2 (Figure 6). Since this same N−H would form a hydrogen bond with L54 of MDM2 upon binding, the water network actually inhibits peptide binding, and the structured water molecules have to be released prior to binding of Stapled. When a W23A mutation was made on Stapled, the water chain fails to form (data not shown).

The hydrogen bonding networks of water in hydrophobic interfaces are very sensitive to changes to its surroundings. One can potentially manipulate the nature of the interface to influence interface water networks and hence alter overall binding energy and kinetics.[64] Additionally, these observations are likely important in developing our general understanding of the role of water on interacting hydrophobic surfaces and hence will be further explored elsewhere.

Implications of the MDM2 Lid on Peptide Binding. The unstructured N-terminal region of MDM2, also known as the "lid", is involved in regulating p53-binding to MDM2.[65,66] Due to the highly dynamic nature of the lid, its structural role in ligand binding regulation is not very well understood. Recent molecular dynamics studies,[67,68] together with NMR analyses, suggest that the lid interconverts between "closed" and "open" states.[65,66] In the "closed" form, the lid interacts with the p53-binding pocket of MDM2,[65,66] thereby occluding the pocket from interacting with p53. The lid is highly flexible when adopting the "open" state, and the hydrophobic pocket of MDM2 is free to interact with any peptide or small molecule drug. Upon binding to p53, the MDM2 lid shifts toward a predominantly "open" conformation.[66] The dynamic equilibrium between the "closed" and "open" conformations depends on phosphorylation, hence opening more possibilities for the lid to regulate MDM2 interactions.[67−69]

In this current study, we have neglected the effects of the MDM2 lid, due to the complexities in modeling a highly dynamic and flexible chain. Effectively, we have considered the

case where the lid is in the "open" conformation, and the hydrophobic pocket is available for peptide binding. This is consistent with the "extended conformational selection" model recently proposed for the MDM2 lid:[67] peptide binding conformationally selects the "open" conformation, and the dynamic equilibrium of MDM2 lid conformations shifts from the predominantly "closed" conformation to a mainly "open" one.

The MDM2 lid may further affect the kinetics and dwell time of the peptides by directly interacting with the peptides as they approach, or when the peptides are bound to the hydrophobic pocket. Understanding these dynamics is critical in our overall understanding of regulatory functions of the MDM2 lid and could lead to future design of stapled peptides and small molecule drugs with specificities that leverage on MDM2 lid dynamics. For instance, when Nutlin is bound to MDM2, the conformational equilibrium of the MDM2 lid is identical to that of apo-MDM2,[66] suggesting perhaps that Nutlin encounters less competition from the lid when binding to MDM2. These effects are being extensively investigated and will be presented elsewhere.

CONCLUSION

Designing therapeutic peptides that target intracellular proteins is a challenging task, with traditional methods typically focused on optimizing the interaction interface between peptide and protein. However, such a strategy could be limited, as noninteracting residues and modifications − such as cyclizations and hydrocarbon staples − could affect the peptide's affinity by modifying the way it approaches the binding pocket. Regular equilibrium simulations do not probe these features.

Here we have explored this question extensively and studied how different peptides − derived from the sequence of p53 TAD − approach and bind to the hydrophobic pocket of MDM2. Identifying small molecules and peptides that inhibit the p53-MDM2 interaction binding is part of the current efforts in oncology research. Our current studies have demonstrated that mutation of key hydrophobic residues (i.e., F19, W23, and/or L26), which have been shown to severely disrupt the binding of p53 peptides, can still lead to MDM2 binding when the peptide is stapled. The interactions between the stapled peptides and MDM2 are facilitated by additional factors that include interactions that the staples make with MDM2 and the organization of water networks around the staples. Furthermore, the malleability of the binding pocket of MDM2 allows for increased promiscuity of interactions between the peptides and the MDM2 hydrophobic pocket. In addition to being a factor that needs to be considered while designing new inhibitors, this also has implications in the search for other MDM2 binding partners[54] − an area of considerable interest given that the MDM2-interaction network will determine the availability of free MDM2 molecules and hence the efficacy of any inhibitor.

Altogether, the observations of this study can assist in the future design of peptides with enhanced binding affinities and peptide dwell times. Additional information that will also greatly aid such development includes the following: details surrounding the entry of stapled peptides into cells; the effects of serum components on the activity of stapled peptides;[25] and the identification of other proteins with binding sites homologous to that of MDM2 in the cell that might interact with the stapled peptides.

ASSOCIATED CONTENT

Supporting Information

The backbone atomic fluctuation of peptide-only simulations; normalized fractional helicity (π and 3_{10}) of peptides in peptide-only simulations; additional histograms of distances between centers of masses in peptide-only simulations; side chain dihedral angles of key hydrophobic residues in peptide-only simulations; time taken for peptides to bind as a function of distance; effect of multiple key residue mutations; changes in binding mechanism due to multiple key residue mutations; table summarizing fitted parameters. This material is available free of charge via the Internet at http://pubs.acs.org.

AUTHOR INFORMATION

Corresponding Authors

*E-mail: adelenes@bii.a-star.edu.sg.
*E-mail: chandra@bii.a-star.edu.sg.

Notes

The authors declare no competing financial interest.

ACKNOWLEDGMENTS

We thank the Verma lab for useful discussions and the A*STAR Computational Resource Centre (A*CRC) for computational resource.

REFERENCES

(1) Vogelstein, B.; Lane, D.; Levine, A. J. *Nature* **2000**, *408*, 307−310.
(2) Zilfou, J. T.; Lowe, S. W. *Cold Spring Harbor Perspect. Biol.* **2009**, *1*, a001883.
(3) Brown, C. J.; Lain, S.; Verma, C. S.; Fersht, A. R.; Lane, D. P. *Nat. Rev. Cancer* **2009**, *9*, 862−873.
(4) Haupt, Y.; Maya, R.; Kazaz, A.; Oren, M. *Nature* **1997**, *387*, 296−299.
(5) Momand, J.; Wu, H. H.; Dasgupta, G. *Gene* **2000**, *242*, 15−29.
(6) Toledo, F.; Wahl, G. M. *Nat. Rev. Cancer* **2006**, *6*, 909−923.
(7) Marine, J. C.; Lozano, G. *Cell Death Differ.* **2010**, *17*, 93−102.
(8) Kussie, P. H.; Gorina, S.; Marechal, V.; Elenbaas, B.; Moreau, J.; Levine, A. J.; Pavletich, N. P. *Science* **1996**, *274*, 948−953.
(9) Wallace, M.; Worrall, E.; Pettersson, S.; Hupp, T. R.; Ball, K. L. *Mol. Cell* **2006**, *23*, 251−263.
(10) Yu, G. W.; Rudiger, S.; Veprintsev, D.; Freund, S.; Fernandez-Fernandez, M. R.; Fersht, A. R. *Proc. Natl. Acad. Sci. U.S.A.* **2006**, *103*, 1227−1232.
(11) Lin, J.; Chen, J.; Elenbaas, B.; Levine, A. J. *Genes Dev.* **1994**, *8*, 1235−1246.
(12) Bottger, A.; Bottger, V.; Garcia-Echeverria, C.; Chene, P.; Hochkeppel, H. K.; Sampson, W.; Ang, K.; Howard, S. F.; Picksley, S. M.; Lane, D. P. *J. Mol. Biol.* **1997**, *269*, 744−756.
(13) Li, C.; Pazgier, M.; Li, C.; Yuan, W.; Liu, M.; Wei, G.; Lu, W. Y.; Lu, W. *J. Mol. Biol.* **2010**, *398*, 200−213.
(14) Secchiero, P.; Bosco, R.; Celeghini, C.; Zauli, G. *Curr. Pharm. Des.* **2011**, *17*, 569−577.
(15) Cheok, C. F.; Verma, C. S.; Baselga, J.; Lane, D. P. *Nat. Rev. Clin. Oncol.* **2011**, *8*, 25−37.
(16) Verdine, G. L.; Hilinski, G. J. *Methods Enzymol.* **2012**, *503*, 3−33.
(17) Verdine, G. L.; Hilinski, G. J. *Drug Discovery Today Technol.* **2012**, *9*, e41−e47.
(18) Verdine, G. L.; Walensky, L. D. *Clin. Cancer Res.* **2007**, *13*, 7264−7270.
(19) Bock, J. E.; Gavenonis, J.; Kritzer, J. A. *ACS Chem. Biol.* **2013**, *8*, 488−499.
(20) Schafmeister, C. E.; Po, J.; Verdine, G. L. *J. Am. Chem. Soc.* **2000**, *122*, 5891−5892.

(21) Walensky, L. D.; Kung, A. L.; Escher, I.; Malia, T. J.; Barbuto, S.; Wright, R. D.; Wagner, G.; Verdine, G. L.; Korsmeyer, S. J. *Science* **2004**, *305*, 1466−1470.
(22) Bernal, F.; Tyler, A. F.; Korsmeyer, S. J.; Walensky, L. D.; Verdine, G. L. *J. Am. Chem. Soc.* **2007**, *129*, 2456−2457.
(23) Kutchukian, P. S.; Yang, J. S.; Verdine, G. L.; Shakhnovich, E. I. *J. Am. Chem. Soc.* **2009**, *131*, 4622−4627.
(24) Baek, S.; Kutchukian, P. S.; Verdine, G. L.; Huber, R.; Holak, T. A.; Lee, K. W.; Popowicz, G. M. *J. Am. Chem. Soc.* **2012**, *134*, 103−106.
(25) Brown, C. J.; Quah, S. T.; Jong, J.; Goh, A. M.; Chiam, P. C.; Khoo, K. H.; Choong, M. L.; Lee, M. A.; Yurlova, L.; Zolghadr, K.; Joseph, T. L.; Verma, C. S.; Lane, D. P. *ACS Chem. Biol.* **2013**, *8*, 506−512.
(26) Joseph, T. L.; Lane, D.; Verma, C. S. *Cell Cycle* **2010**, *9*, 4560−4568.
(27) Joseph, T. L.; Lane, D. P.; Verma, C. S. *PLoS One* **2012**, *7*, e43985.
(28) Stewart, M. L.; Fire, E.; Keating, A. E.; Walensky, L. D. *Nat. Chem. Biol.* **2010**, *6*, 595−601.
(29) Phillips, C.; Roberts, L. R.; Schade, M.; Bazin, R.; Bent, A.; Davies, N. L.; Moore, R.; Pannifer, A. D.; Pickford, A. R.; Prior, S. H.; Read, C. M.; Scott, A.; Brown, D. G.; Xu, B.; Irving, S. L. *J. Am. Chem. Soc.* **2011**, *133*, 9696−9699.
(30) Dastidar, S. G.; Lane, D. P.; Verma, C. S. *Cell Cycle* **2012**, *11*, 2239−2247.
(31) Botuyan, M. V.; Momand, J.; Chen, Y. *Fold. Des.* **1997**, *2*, 331−342.
(32) Lee, H.; Mok, K. H.; Muhandiram, R.; Park, K. H.; Suk, J. E.; Kim, D. H.; Chang, J.; Sung, Y. C.; Choi, K. Y.; Han, K. H. *J. Biol. Chem.* **2000**, *275*, 29426−29432.
(33) Bell, S.; Klein, C.; Muller, L.; Hansen, S.; Buchner, J. *J. Mol. Biol.* **2002**, *322*, 917−927.
(34) Chang, J.; Kim, D. H.; Lee, S. W.; Choi, K. Y.; Sung, Y. C. *J. Biol. Chem.* **1995**, *270*, 25014−25019.
(35) Dawson, R.; Muller, L.; Dehner, A.; Klein, C.; Kessler, H.; Buchner, J. *J. Mol. Biol.* **2003**, *332*, 1131−1141.
(36) Hernychova, L.; Man, P.; Verma, C.; Nicholson, J.; Sharma, C. A.; Ruckova, E.; Teo, J. Y.; Ball, K.; Vojtesek, B.; Hupp, T. R. *Proteomics* **2013**, *13*, 2512−2525.
(37) Gotz, A. W.; Williamson, M. J.; Xu, D.; Poole, D.; Le Grand, S.; Walker, R. C. *J. Chem. Theory. Comput.* **2012**, *8*, 1542−1555.
(38) Salomon-Ferrer, R.; Goetz, G. W.; Poole, D.; Le Grand, S.; Walker, R. C. *J. Chem. Theory Comput.* **2013**, *9*, 3878−3888.
(39) Case, D. A.; Darden, T.; Cheatham, T., III; Simmerling, C. L.; Wang, J.; Duke, R. E.; Luo, R.; Walker, R. C.; Zhang, W.; Merz, K. M.; Roberts, B.; Hayik, S.; Roitberg, A.; Seabra, G.; Swails, J.; Goetz, A. W.; Kolossváry, I.; Wong, K. F.; Paesani, F.; Vanicek, J.; Wolf, R. M.; Liu, J.; Wu, X.; Brozell, S. R.; Steinbrecher, T.; Gohlke, H.; Cai, Q.; Ye, X.; Wang, J.; Hsieh, M. J.; Cui, G.; Roe, D. R.; Mathews, D. H.; Seetin, M. G.; Salomon-Ferrer, R.; Sagui, C.; Babin, V.; Luchko, T.; Gusarov, S.; Kovalenko, A.; Kollman, P. A. *AMBER 12*; University of California: San Francisco, 2012.
(40) Hornak, V.; Abel, R.; Okur, A.; Strockbine, B.; Roitberg, A.; Simmerling, C. *Proteins* **2006**, *65*, 712−725.
(41) Jorgensen, W. L.; Chandrasekhar, J.; Madura, J. D.; Impey, R. W.; Klein, M. L. *J. Chem. Phys.* **1983**, *79*, 926−935.
(42) Darden, T.; York, D.; Pedersen, L. *J. Phys. Chem.* **1993**, *98*, 10089−10092.
(43) Ryckaert, J.-P.; Ciccotti, G.; Berendsen, H. J. C. *J. Comput. Phys.* **1977**, *23*, 327−341.
(44) The PyMOL Molecular Graphics System, V. r. p., Schrödinger, LLC.
(45) Guo, Z.; Mohanty, U.; Noehre, J.; Sawyer, T. K.; Sherman, W.; Krilov, G. *Chem. Biol. Drug Des.* **2010**, *75*, 348−359.
(46) Dastidar, S. G.; Madhumalar, A.; Fuentes, G.; Lane, D. P.; Verma, C. S. *Theor. Chem. Acc.* **2009**, *125*, 621−635.
(47) ElSawy, K. M.; Verma, C. S.; Joseph, T. L.; Lane, D. P.; Twarock, R.; Caves, L. S. *Cell Cycle* **2013**, *12*, 394−404.
(48) Garcia-Echeverria, C.; Chene, P.; Blommers, M. J.; Furet, P. *J. Med. Chem.* **2000**, *43*, 3205−3208.
(49) Kallen, J.; Goepfert, A.; Blechschmidt, A.; Izaac, A.; Geiser, M.; Tavares, G.; Ramage, P.; Furet, P.; Masuya, K.; Lisztwan, J. *J. Biol. Chem.* **2009**, *284*, 8812−8821.
(50) Schon, O.; Friedler, A.; Bycroft, M.; Freund, S. M.; Fersht, A. R. *J. Mol. Biol.* **2002**, *323*, 491−501.
(51) Joseph, T. L.; Madhumalar, A.; Brown, C. J.; Lane, D. P.; Verma, C. S. *Cell Cycle* **2010**, *9*, 1167−1181.
(52) Vassilev, L. T.; Vu, B. T.; Graves, B.; Carvajal, D.; Podlaski, F.; Filipovic, Z.; Kong, N.; Kammlott, U.; Lukacs, C.; Klein, C.; Fotouhi, N.; Liu, E. A. *Science* **2004**, *303*, 844−848.
(53) Bista, M.; Wolf, S.; Khoury, K.; Kowalska, K.; Huang, Y.; Wrona, E.; Arciniega, M.; Popowicz, G. M.; Holak, T. A.; Domling, A. *Structure* **2013**, *21*, 2143−2151.
(54) Nicholson, J.; Neelagandan, K.; Huart, A. S.; Ball, K.; Molloy, M. P.; Hupp, T. *J. Proteome Res.* **2012**, *11*, 5464−5478.
(55) Ball, P. *Chem. Rev.* **2008**, *108*, 74−108.
(56) Chaplin, M. *Nat. Rev. Mol. Cell Biol.* **2006**, *7*, 861−866.
(57) Ball, P. *Nature* **2003**, *423*, 25−26.
(58) Chandler, D. *Nat. Cell Biol.* **2005**, *437*, 640−647.
(59) Liu, P.; Huang, X.; Zhou, R.; Berne, B. J. *Nature* **2005**, *437*, 159−162.
(60) Zhou, R.; Huang, X.; Margulis, C. J.; Berne, B. J. *Science* **2004**, *305*, 1605−1609.
(61) Sun, T.; Lin, F. H.; Campbell, R. L.; Allingham, J. S.; Davies, P. L. *Science* **2014**, *343*, 795−798.
(62) Teeter, M. M. *Proc. Natl. Acad. Sci. U.S.A.* **1984**, *81*, 6014−6018.
(63) Head-Gordon, T. *Proc. Natl. Acad. Sci. U.S.A.* **1995**, *92*, 8308−8312.
(64) Patel, A. J.; Varilly, P.; Jamadagni, S. N.; Hagan, M. F.; Chandler, D.; Garde, S. *J. Phys. Chem. B* **2012**, *116*, 2498−2503.
(65) McCoy, M. A.; Gesell, J. J.; Senior, M. M.; Wyss, D. F. *Proc. Natl. Acad. Sci. U.S.A.* **2003**, *100*, 1645−1648.
(66) Showalter, S. A.; Bruschweiler-Li, L.; Johnson, E.; Zhang, F.; Bruschweiler, R. *J. Am. Chem. Soc.* **2008**, *130*, 6472−6478.
(67) Verkhivker, G. M. *PLoS One* **2012**, *7*, e40897.
(68) Dastidar, S. G.; Raghunathan, D.; Nicholson, J.; Hupp, T. R.; Lane, D. P.; Verma, C. S. *Cell Cycle* **2011**, *10*, 82−89.
(69) Worrall, E. G.; Wawrzynow, B.; Worrall, L.; Walkinshaw, M.; Ball, K. L.; Hupp, T. R. *J. Chem. Biol.* **2009**, *2*, 113−129.